Available online at www.sciencedirect.com
ScienceDirect
Trans. Nonferrous Met. Soc. China 23(2013) 1922−1929
Transactions of Nonferrous Metals Society of China
www.tnmsc.cn

Creep age forming of 2124 aluminum alloy with single/double curvature

Jin ZHANG, Yun-lai DENG, Si-yu LI, Ze-yu CHEN, Xin-ming ZHANG
School of Materials Science and Engineering, Central South University, Changsha 410083, China

Received 25 September 2012; accepted 19 December 2012

Abstract: In order to investigate the springback rules, the variation characteristics of physical property and microstructure in bending creep age forming process, a series of creep forming tests of 2124 aluminum alloy were conducted based on three kinds of single and double curvature forming tools. The results show that the spingback rate would be the minimum under the optimal coupling conditions among the temperature, aging time and internal stress state of material. Difference exists in the two directions of the formed sample with double curvature, but the curvature variation keeps the same. Yield strength, ultimate tensile strength and fracture toughness of the double curvature formed sample appear to be higher than those of the single curvature formed sample under the same aging condition, but the elongation and the anisotropy are opposite.
Key words: springback; creep age forming; double curvature bending; 2124 aluminum alloy

1 Introduction

Creep age forming (CAF), a novel process which combines age-hardening and stress-induced deformation, has been developed rapidly due to the increasing demands in aerospace industry for manufacturing large integrally stiffened lightweight panels [1−4]. Compared with the other conventional plastic forming methods, CAF has the main advantages of the material safety and the repeatable process, as well as the ability to produce components with complicated curved surface. In the CAF process, after the solution treated component is loaded onto the tool surface, it is kept at certain aging condition, then the part is released and partially springbacks to a shape somewhere between its original shape and the tool shape [5, 6]. This phenomenon occurs due to the stress relaxation and the microstructure variation during the coupled thermo-mechanical process [7−9]. Therefore, a large number of studies on spingback law, mechanical properties and microstructure of alloys are necessary to establish a balance among them. Several relevant investigations have been reported so far. DENG et al [10] investigated the characteristics of microstructure and property in creep aging process of 2124 aluminum alloy. CHEN et al [11] investigated the effects of temperature on the creep behavior of 2024 aluminum alloy. ARABI et al [12] investigated the effects of time and temperature on the creep forming of 7075 aluminum alloy. To predict the springback, many creep constitutive models [13−15] have been established for different kinds of aluminum alloys, and the constitutive relations have been considered along with the mechanical properties. However, these are merely based on uniaxial tensile tests and single curvature tools. As for the CAF process with more complex tool shape, such as double curvature, the corresponding basic researches are limited in the literatures yet.

In this work, CAF experiments of 2124 aluminum alloy were designed with self-made single/double curvature forming tools, and corresponding tests were conducted on spingback, mechanical properties and microstructure of the formed samples.

2 Experimental

2.1 Tools and specimens

Hot rolled sheets of 2124 Al alloy with the dimensions of 230 mm×130 mm×5 mm were used in this study, and the chemical composition is presented in Table 1. The structure and components of the prepared forming tools are shown in Fig. 1. The sheet specimens used in the CAF experiments could be classified into three types according to the tool surface: the first kind

Foundation item: Project (2010CB731700) supported by the National Basic Research Program of China
Corresponding author: Yun-lai DENG; Tel: +86-731-88876931; E-mail: luckdeng@csu.edu.cn
DOI: 10.1016/S1003-6326(13)62678-3

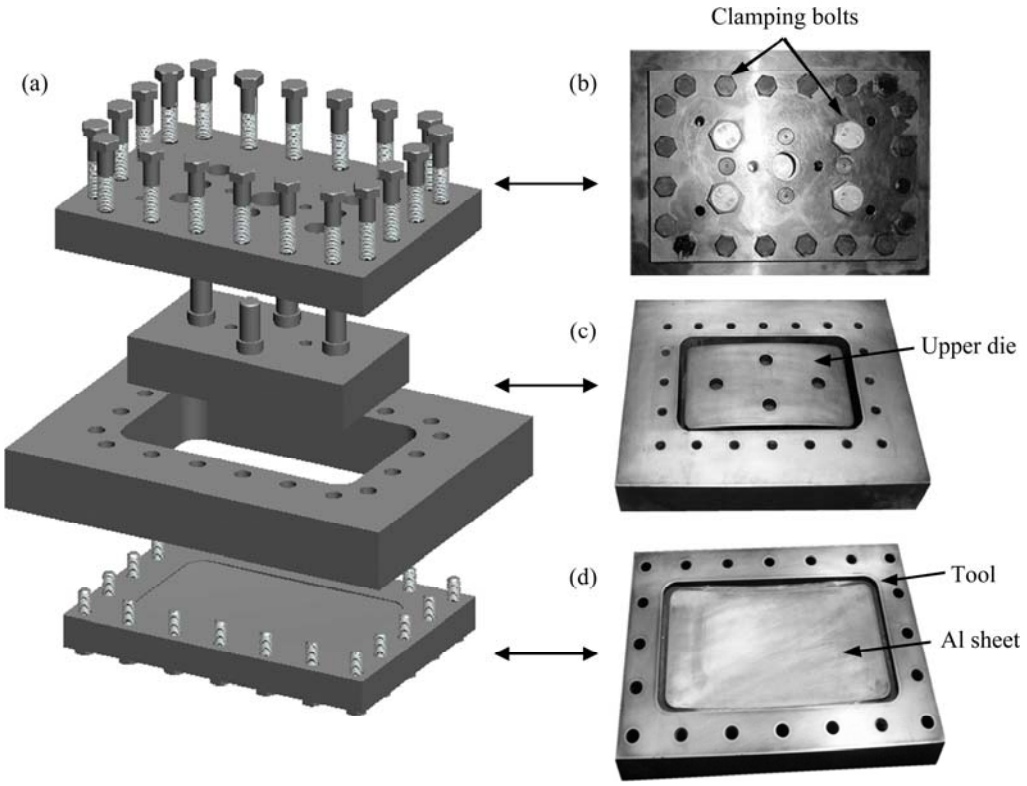

Fig. 1 Schematic illustration of creep forming tools: (a) Assembly diagram of tool parts; (b) Fixing plate and clamping bolts; (c) Upper die; (d) Al sheet on tool surface

Table 1 Chemical composition of 2124 alloy (mass fraction, %)

Cu	Mg	Mn	Ti	Zn
4.18	1.46	0.52	0.028	0.03
Cr	Fe	Si	Al	
0.003	0.22	0.11	Bal.	

of sheet was used in the single curvature tool with a curvature radius along the length direction R_1=1000 mm (denoted as SCAF); the second kind was used in the double curvature tool with a curvature radius along the long direction R_1=1000 mm and along the width direction R_2=2000 mm (denoted as DCAF); the third kind was used in the double curvature tool with R_1=3000 mm and R_2=6000 mm (denoted as RDCAF).

2.2 Heat treatments

After being solution treated at 495 °C for 45 min and water quenched, the hardness values of the 2124 aluminum alloy samples when exposed at different temperatures for different intervals of time are shown in Fig. 2. A dominant trend can be observed for all of the samples and all of the aging conditions: the hardness goes up as the aging time and temperature increase, and further increase in the aging time results in a maximum after which the hardness decreases. It can also be known that the first time to reach the maximum hardness at

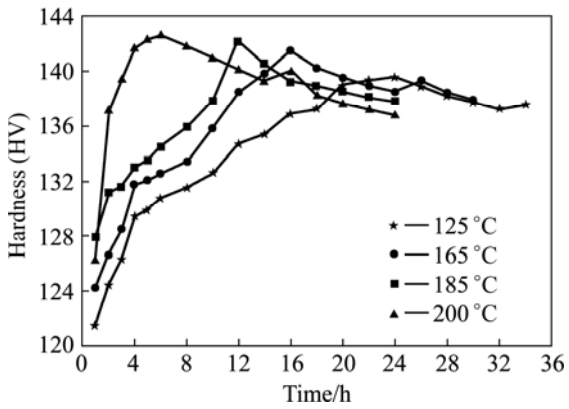

Fig. 2 Hardness of 2124 Al alloy following change of aging time at different temperatures

temperature of 125, 165, 185 and 200 °C are 24, 16, 12 and 6 h respectively. For this reason, the four peak aging conditions were chosen to the CAF experiments of 2124 aluminum alloy sheets based on the aforementioned forming tools.

2.3 Overall experimental procedure

The experimental procedure, as shown in Fig. 3, can be described as follows. After being solution treated and water quenched, the specimens were kept at a refrigerated condition to reduce natural aging. Subsequently, the sheet specimen was mounted on the

tool and was then clamped using bolts (Fig.1 (b)). Then, the whole assembly was placed in the furnace and the creep aging process started. After aging for a certain time, the heating was switched off, the furnace was opened and the load was removed. The CAF process could also be divided into three steps: in the first stage, the specimen was elastically loaded onto the tool surface; then the specimen kept its shape during the aging process, and the combined effect of stress relaxation due to creep and age hardening due to precipitation acted until the end of the second stage; in the last stage, the specimen was retrieved and could not return to its initial shape for the effect from the previous stage, as shown in Fig. 4.

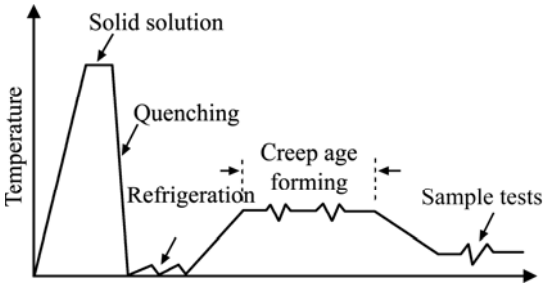

Fig. 3 Schematic drawing of experimental process

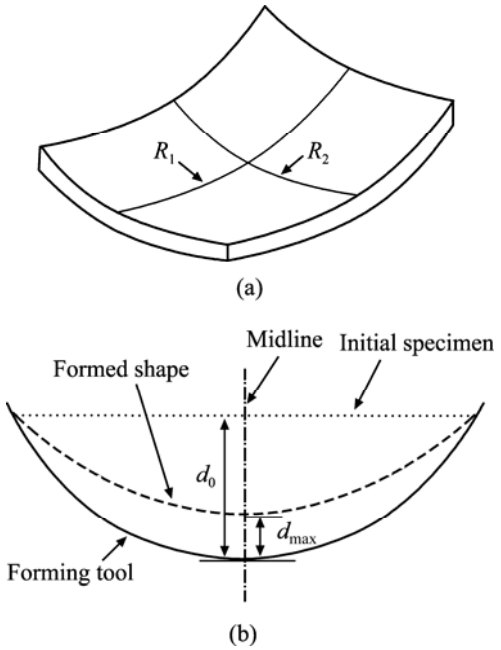

Fig. 4 Schematic drawing of double curvature bending (a) and springback (b)

2.4 Test methods

The definition of the springback is quantified by a factor according to

$$\eta = (d_{max} / d_0) \times 100\% \quad (1)$$

where d_0 is the maximum vertical distance between the initial specimen and the forming tool surface, and d_{max} is the maximum vertical distance between the formed shape and the forming tool surface, as shown in Fig. 4.

Tensile tests in the rolling direction were carried out at room temperature using the CSS−44100 machine operating at a constant crosshead speed of 2 mm/min. Transmission electron microscopy (TEM) was used to characterize the precipitates under different forming conditions. Samples for TEM observation were mechanically thinned down to 80 μm and electropolished using a twin-jet polisher with a 30% nitric acid solution in methanol maintained at −30 °C and 20 V. The foils were observed by using TECNAIG220 transmission electron microscope and images were taken on several places of the specimen. In accordance with ASTM B871-01, fracture toughness was measured by the Kahn tear test, using the MTS810 dynamic fatigue testing machine with a stretching speed of 1 mm/min. Then the fracture toughness could be characterized by the unit initiation energy (UIE) [16]. The different fracture morphology of the tore specimens were examined by image analysis of SEM micrographs.

3 Results and discussion

3.1 Springback

Figure 5 shows the measured springback results of the CAF experiments. Figure 5(a) illustrates the springback of the DCAF sample along the length and width directions under four different aging conditions. It was observed that the maximum hardness increased as a result of increasing temperature, as shown in Fig. 2. However, the springback of the samples did not change monotonically, but instead in a decrease-to-increase manner. Both the length and width directions had the minimum springback at the aging condition of (185 °C, 12 h), which are 18.5% and 15% lower than the maximum under each direction respectively. This indicates that the amount of springback is obviously influenced by the aging conditions.

The springback of the RDCAF sample along the length and width directions at four different aging conditions are illustrated in Fig. 5(b). Combining with Fig. 5(a), some common characters exist in the CAF samples formed by tools with different curvatures. First, at the same aging condition, the maximum difference of springback value between the length direction (R_1=1000 mm) and the width direction (R_1=2000 mm) could reach 20% for the DCAF samples, and 8% for the RDCAF samples. The springback values of the RDCAF samples are generally less than those of the DCAF samples. It is thus clear that the springback can be obviously influenced by the internal stress state of material, which depends on the curvatures of different forming dies or different directions in the same die. Second, as the aging

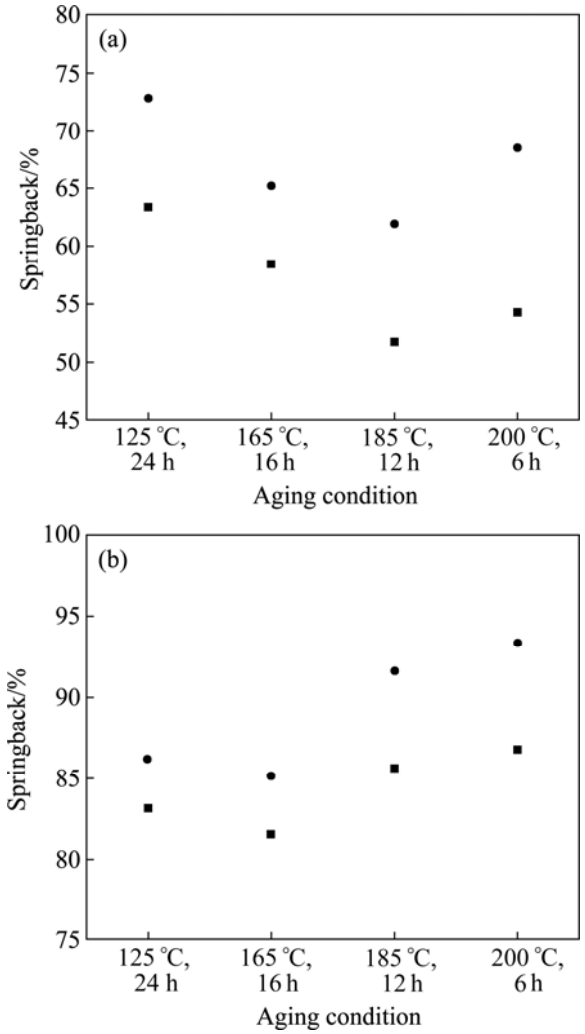

Fig. 5 Relationship between springback and aging regime with different double curvature dies: (a) R_1=1000 mm, R_2=2000 mm; (b) R_1=3000 mm, R_2=6000 mm

condition changes, the springback variations of the samples with different curvatures have the same trend, that is, decreasing first and then increasing as the aging temperature increases. Moreover, interactive coordination exists in the two directions of DCAF and RDCAF samples for different springback values. This can be proved by the nearly parallel curves of springback in the two directions, as shown in Figs. 5(a) and (b).

Comparing Fig. 5(a) with 5(b), it can be seen that the springback value reaches the minimum at the aging condition of (185 °C, 12 h) for the DCAF samples, but (165 °C, 16 h) for the RDCAF samples. This difference denotes that the plastic strain in CAF process is related to not only the aging conditions, but also the internal stress state of material, which means interior bending stress here. And the springback value of the sheet specimens would be the minimum if the two factors reach the optimal coupling state. In other words, if the die surface has been determined, there must be an aging condition to make a minimum springback.

The springback values of the SCAF and DCAF samples along the length direction under four different aging conditions are compared in Fig. 6. It is observed that the springback variations of the two samples have the same trend and reach the minimum under the same aging condition of (185 °C, 12 h). The springback of the DCAF sample is obviously lower than that of the SCAF sample. For example, the springback along the length direction of the DCAF sample is 51.7% at the aging condition of (185 °C, 12 h), which is 7% lower than that of the SCAF sample. Combining the results shown in Fig. 5(a), it can be inferred that both the two directions of the DCAF sample restrict and coordinate each other, which render the springback lower than the corresponding SCAF samples. Just because of this, although the springback along the width direction is higher than that along the length direction, the springback along the length direction of the DCAF sample is still reduced.

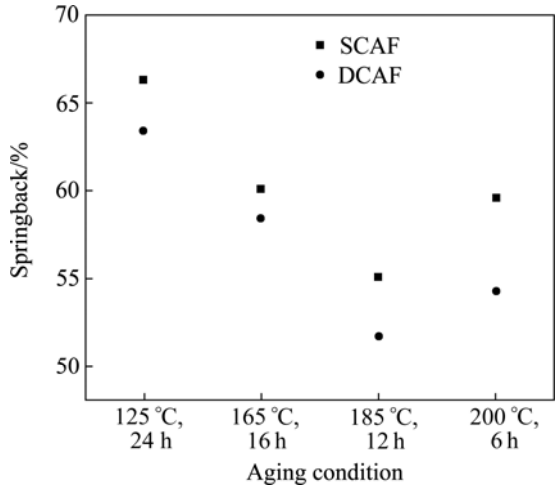

Fig. 6 Relationship between springback and aging condition with single or double curvature die

3.2 Mechanical properties

Figure 7 illustrates the mechanical properties of the SCAF and DCAF specimens at the directions of 0°, 45° and 90° from the rolling direction. It can be observed that both the SCAF and DCAF specimens have a similar variation characteristic and reach the maximum yield strength and ultimate tensile strength at the same aging condition of (185 °C, 12 h). However, the yield strength and ultimate tensile strength of the DCAF specimens appear to be higher than those of the SCAF specimens, as shown in Figs. 7(a) and (b). As shown in Fig. 7(c), the maximum elongation exists at the aging condition of (125 °C, 24 h), and the elongation of the DCAF specimens is slightly lower than that of the SCAF specimens. Obvious anisotropy can be seen in the mechanical properties along the three directions, and both the yield strength and the ultimate tensile strength

follow the rule of $\sigma_{0°}>\sigma_{90°}>\sigma_{45°}$, but the elongation is reversed.

3.3 Microstructures

The microstructures of the 2124 alloy after artificial aging, SCAF and DCAF at the same heat treatment of (185 °C, 12 h) were examined using TEM, as illustrated in Fig. 8. In the order of artificial aging, SCAF and DCAF, it can be seen that the precipitate size gradually becomes finer and the distribution becomes denser. These changes could strengthen the age hardening effect of the alloy [17], so the yield strength of the DCAF specimen is higher than that of the SCAF specimen, which is consistent with Fig. 7(a).

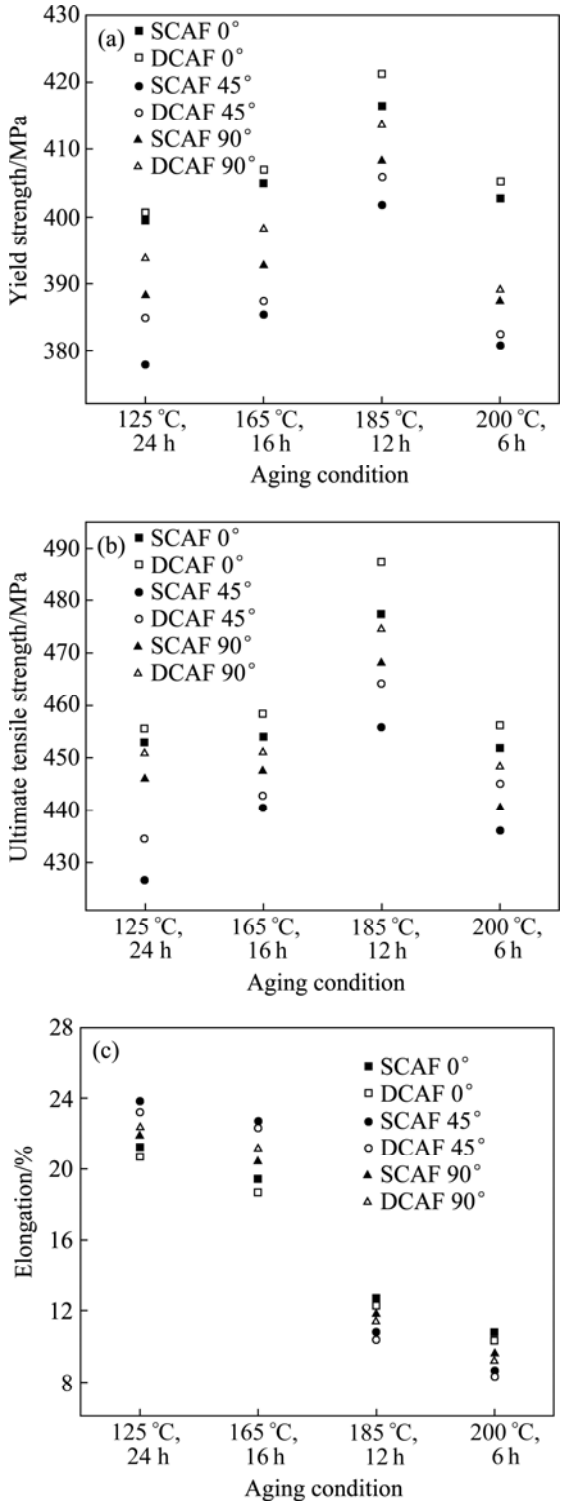

Fig. 7 Mechanical properties of creep formed 2124 Al sheet specimens with single/double curvature: (a) Yield strength; (b) Ultimate tensile strength; (c) Elongation

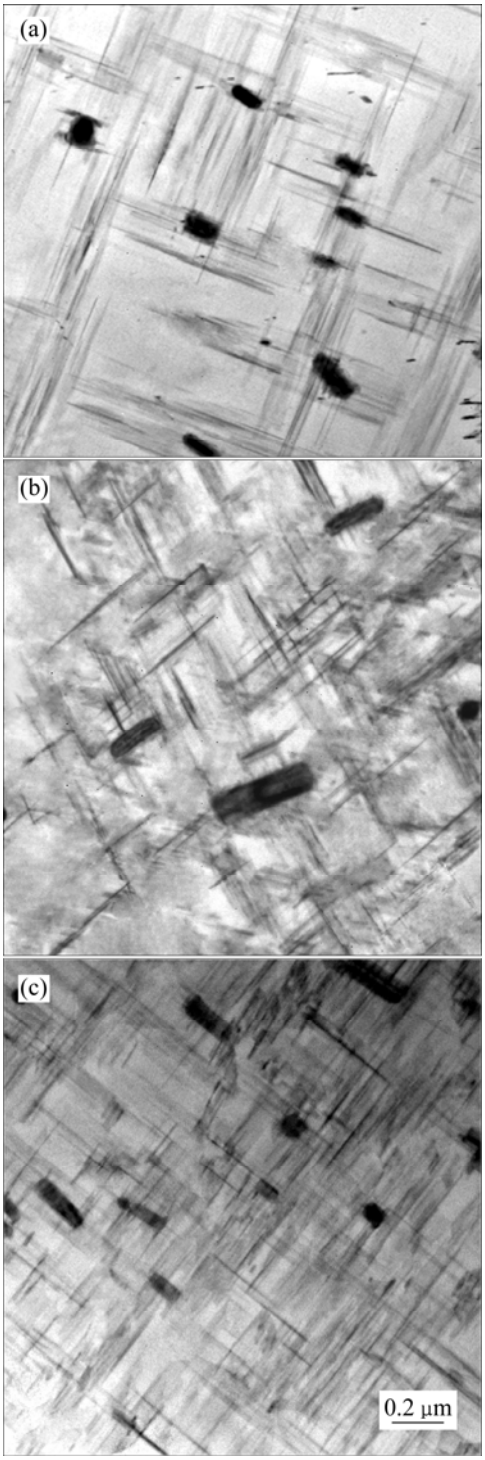

Fig. 8 TEM images of 2124 Al specimens: (a) Artificial aged; (b) SCAF under aging condition of (185 °C, 12 h); (c) DCAF under aging condition of (185 °C, 12 h)

3.4 Fracture toughness

Figure 9 shows the unit initiation energy (UIE) values of the SCAF and DCAF specimens at the directions of 0°, 45° and 90° from the rolling direction. It can be known that the UIE decreases with the increasing of heat treatment temperature, and the UIE values at the heat treatment of (185 °C, 12 h) and (200 °C, 6 h) are very close. Obvious anisotropy can be seen in the UIE along the three directions, following the rule of $UIE_{45°}$> $UIE_{90°}$>$UIE_{0°}$. And it also can be known that the fracture toughness of the DCAF specimens appears to be higher than that of the SCAF specimens.

SEM fractographs of the SCAF specimens under different aging conditions are shown in Fig. 10. It can be observed that these fracture surfaces are mainly composed of ductile transgranular fracture and ductile intergranular fracture. As the heat treatment temperature increases, the dominating fracture type changes from the ductile transgranular fracture to the ductile intergranular fracture. It means that the toughness of the alloy would reduce [16], which is consistent with the variation of UIE, as shown in Fig. 9. The same characteristics also exist in the DCAF specimens, as shown in Fig. 11.

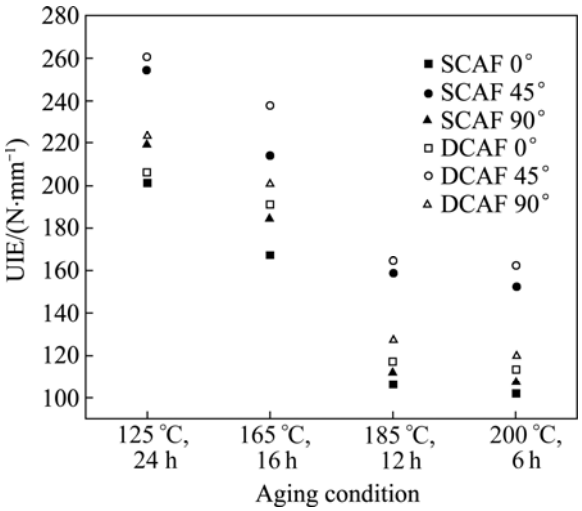

Fig. 9 UIE of SCAF and DCAF specimens at directions of 0°, 45° and 90° from rolling direction

3.5 Anisotropy

The degree of anisotropy is here referred to as "in-plane anisotropy" (IPA) [18], which is defined as

$$\mathrm{IPA}=\frac{2X_{\max}-X_{\mathrm{med}}-X_{\min}}{2X_{\max}}\times 100\% \quad (2)$$

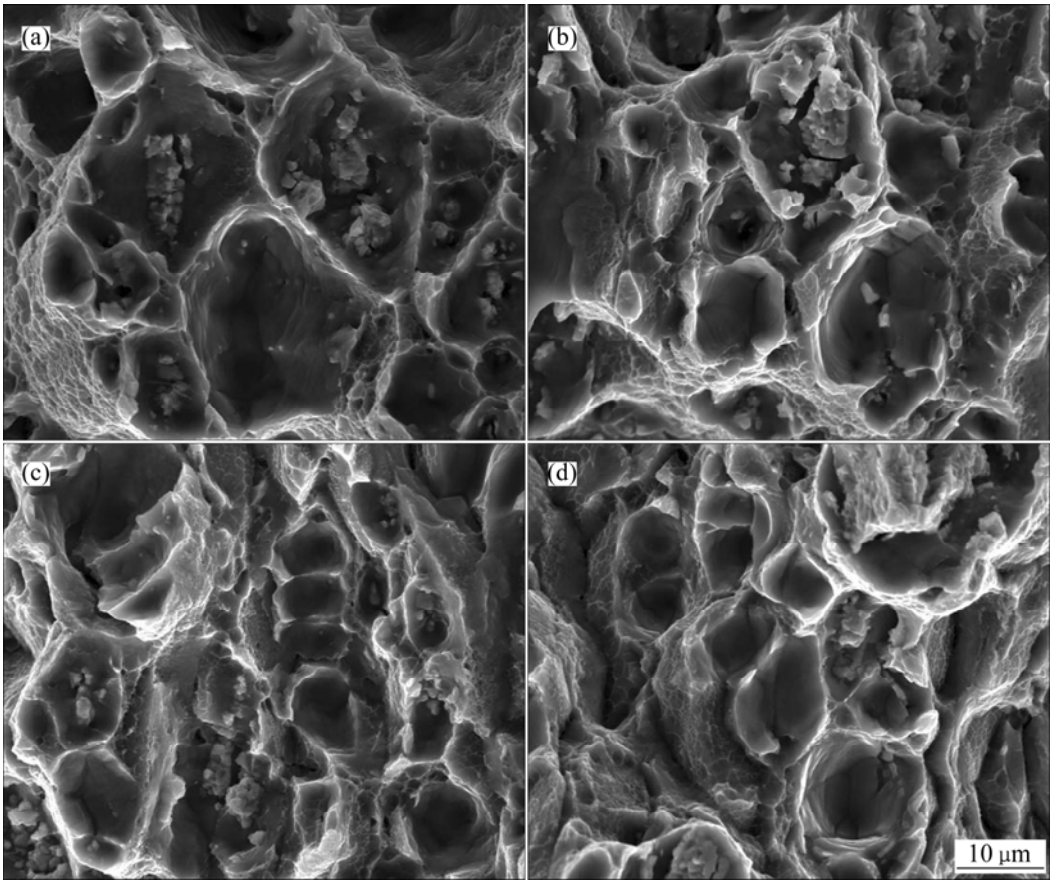

Fig. 10 SEM fractographs of SCAF specimens under different aging conditions: (a) 125 °C, 24 h; (b) 165 °C, 16 h; (c) 185 °C, 12 h; (d) 200 °C, 6 h

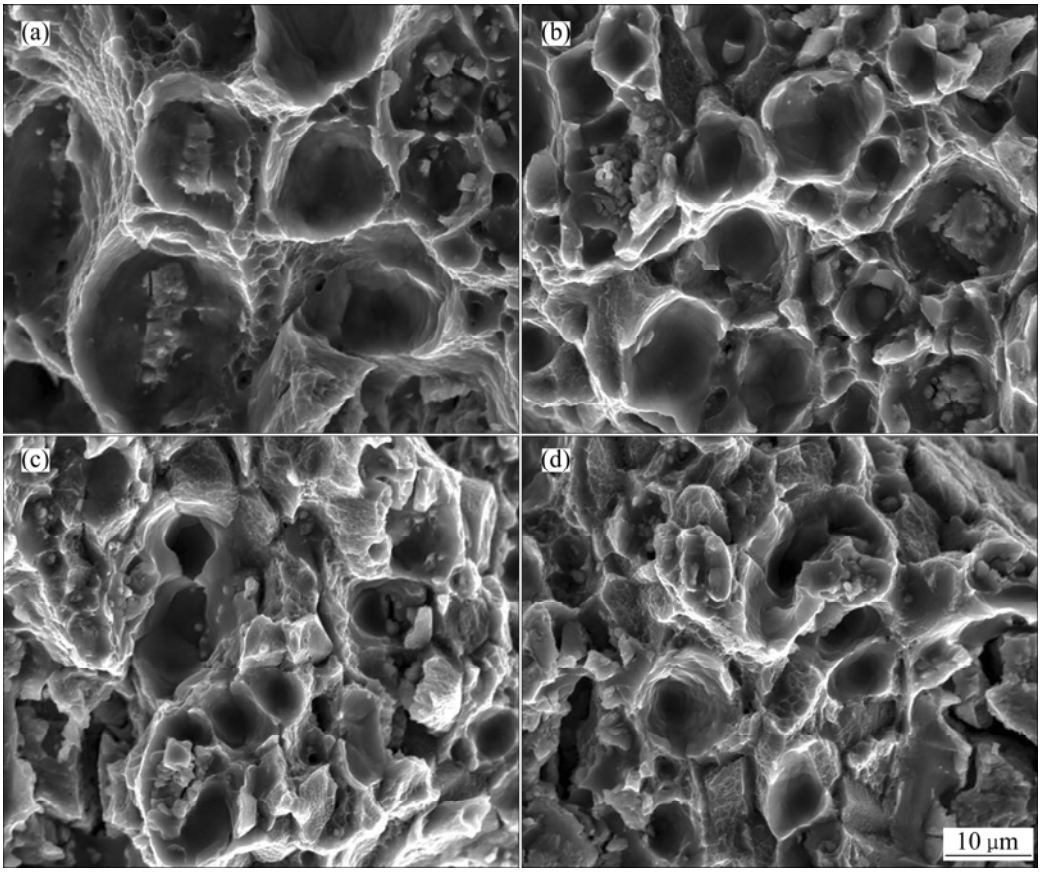

Fig. 11 SEM fractographs of DCAF specimens under different aging conditions: (a) 125 °C, 24 h; (b) 165 °C, 16 h; (c) 185 °C, 12 h; (d) 200 °C, 6 h

where X_{max}, X_{med} and X_{min} represent the maximum, median and minimum of a factor at the directions of 0°, 45° and 90° from the rolling direction. According to Eq. (2), the IPA of ultimate strength, elongation and UIE of SCAF and DCAF specimens under the four aging conditions were calculated, as shown in Fig. 12. It can be observed that the IPA of the ultimate tensile strength is the highest, UIE the lowest, and the elongation in the middle. More importantly, all three kinds of IPA of the DCAF specimens are consistently lower than those of the SCAF specimens.

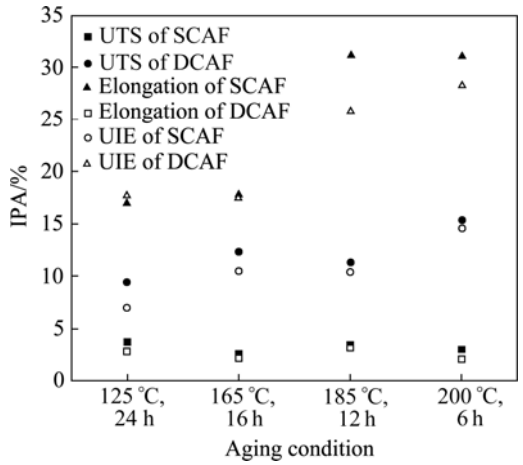

Fig. 12 IPA of ultimate tensile strength, elongation and UIE of SCAF and DCAF specimens under different aging conditions

4 Conclusions

1) Springback is obviously influenced by the aging condition, and also related to the internal stress state of material. The springback value of the sheet specimens would be the minimum if the two factors reach the optimal coupling state.

2) Obvious difference exists in the two directions of double curvature shaped tools, but their interactive coordination could cause the nearly parallel curves of springback in the two directions and certain restrictions on the springback.

3) Yield strength and ultimate tensile strength of the DCAF specimens appear to be higher than those of the SCAF specimens at the same aging condition, but the elongation is reversed.

4) The degree of anisotropy of ultimate tensile strength is the highest, UIE the lowest, and elongation in the middle. And all three kinds of IPA of the DCAF specimens are consistently lower than those of the SCAF specimens.

References

[1] WILLIAMS J C, STARKE E A. Progress in structural materials for aerospace systems [J]. Acta Materialia, 2003, 51(19): 5775−5799.

[2] HO K C, LIN J, DEAN T A. Modelling of springback in creep forming thick aluminum sheets [J]. International Journal of Plasticity, 2004, 20(4−5): 733−751.

[3] JEUNECHAMPS P P, HO K C, LIN J. A closed form technique to predict springback in creep age-forming [J]. International Journal of Mechanical Sciences, 2006, 48(6): 621−629.

[4] HEINZ A, HASZLER A, KEIDEL C. Recent development in aluminium alloys for aerospace applications [J]. Materials Science and Engineering A, 2000, 280(1): 102−107.

[5] HO K C, LIN J, DEAN T A. Constitutive modelling of primary creep for age forming an aluminium alloy [J]. Journal of Materials Processing Technology, 2004, 153−154: 122−127.

[6] LIN J, HO K C, DEAN T A. An inergrated process for modelling of precipitation hardening and springback in creep age-forming [J]. International Journal of Machine Tools and Manufacture, 2006, 46(11): 1266−1270.

[7] ZHAN L H, LIN J, DEAN T A. Experimental studies and constitutive modelling of the hardening of aluminium alloy 7055 under creep age forming conditions [J]. International Journal of Mechanical Sciences, 2011, 53(8): 595−605.

[8] LI K P, CARDEN W P, WAGONER R H. Simulation of springback [J]. International Journal of Mechanical Sciences, 2002, 44(1): 103−122.

[9] DU X D. Study on ageing and creep of Al−0.1Zr alloy [J]. Materials Science and Engineering A, 2006, 432(1−2): 84−89.

[10] DENG Yun-lai, ZHOU Liang, JIN Kun, ZHANG Xin-ming. Microstructure and properties of creep aged 2124 aluminum alloy [J]. The Chinese Journal of Nonferrous Metals, 2010, 20(11): 2106−2111. (in Chinese)

[11] CHEN Yu-qiang, YI Dan-qing, PAN Su-ping. Effect of temperature on creep behavior of 2024 aluminum alloy [J]. The Chinese Journal of Nonferrous Metals, 2010, 20(4): 632−639. (in Chinese)

[12] ARABI J R, EMAMI M, SHAHVERDI H R. Effects of time and temperature on the creep forming of 7075 aluminum alloy: Springback and mechanical properties [J]. Materials Science and Engineering A, 2011, 528(29−30): 8795−8799.

[13] LI Chao, WAN Min, WU Xiang-dong, HUANG Lin. Constitutive equations in creep of 7B04 aluminum alloys[J]. Materials Science and Engineering A, 2010, 527(16−17): 3623−3629.

[14] WANG J F, WAGONER R H, CARDEN W D. Creep and anelasticity in the springback of aluminum [J]. International Journal of Plasticity, 2004, 20(12): 2209−2232.

[15] ZHAN Li-hua, LIN Jian-guo, DEAN T A. A review of the development of creep age forming: Experimentation, modelling and applications [J]. International Journal of Machine Tools and Manufacture, 2011, 51(1): 1−17.

[16] DUMONT D, DESCHAMPS A, BRECHET Y. On the relationship between microstructure, strength and toughness in AA7050 aluminum alloy [J]. Materials Science and Engineering A, 2003, 356(1−2): 326−336.

[17] LIU Gang, DING Xiang-dong, SUN Jun. A model for age strengthening of plate-like-precipitate-containing Al alloys [J]. The Chinese Journal of Nonferrous Metals, 2001, 11(3): 337−346. (in Chinese)

[18] JATA K V, HOPKINS A K, RIOJA R J. The anisotropy and texture of Al−Li alloys [J]. Materials Science Forum, 1996, 217−222: 647−652.

2124 铝合金的单、双曲率蠕变时效成形

张 劲，邓运来，李思宇，陈泽宇，张新明

中南大学 材料科学与工程学院，长沙 410083

摘 要：为了研究弯曲蠕变时效成形过程中的回弹规律以及物理性能与微观结构的演变特征，基于 3 种单曲率模具和双曲率模具，以 2124 铝合金为研究对象，选取 4 种不同温度的峰值时效制度进行一系列的蠕变时效成形试验。结果表明：当时效温度、时间和材料内部应力状态达到最佳耦合效果时，板材的回弹率达到最小。双曲率蠕变成形试样在两个方向上的回弹率存在明显差异，但能够保持一致的变化规律。在同样的时效制度下，双曲率蠕变成形后试样的屈服强度、抗拉强度和断裂韧性均要高于单曲率蠕变成形的，而伸长率与各向异性则相反。

关键词：回弹；蠕变时效成形；双曲率弯曲；铝合金

(Edited by Sai-qian YUAN)